Electron density measurement from the emissivity ratio in hyperbolic geometry resampling the divertor of fusion reactor tokamak

Awad S. Alhasi

Department of Physics, Faculty of Science, University of Benghazi, Benghazi, Libya

Alhasiawad@gmail.com:

Highlights

- **The plasma intensity $\phi(y)$ is measured to obtain the plasma emissivity $\epsilon(\psi)$ as function of the magnetic flux coordinate ψ,**
- **Taken the emissivity ratio for the H_β and H_γ lines, the electrons' temperature is calculated.**
- **The plasma electrons density is inferred from the calculated temperature.**

ARTICLE INFO

ABSTRACT

The aim of this paper is to secure formula for measuring the electron density of the inhomogeneous plasma in divertor of the future reactor tokamaks such as the International Thermonuclear Experimental Reactor (ITER). This is done firstly by determining the emissivity ratio of the H_β and H_γ lines of hydrogen plasma to get the electron temperature. Secondly, we use the resulting temperature to infer the electron density. The emissivity ratio is obtained by hyperbolic inversion of the measured intensity of the H_β and H_γ lines. It is assumed that the free electrons have a Maxwellian velocity distribution and that the distribution of electron population over the bound levels is given by a coronal-type equation. The hydrogen plasma is assumed to be in a steady state without impurities contributing to the electron density.

1. Introduction

This work is devoted to the electron plasma density measurement, where electron's temperature is obtained by the emissivity ratio form which the electrons density is inferred. The line emissivity ratio method for measuring the electron temperature of a homogeneous plasma in Local Thermodynamic Equilibrium (LTE) is well established (Alhasi, 2007). The distribution of electron population over the bound and free states for these plasmas and the distribution of ions species are given by the Boltzmann and Saha equations. The temperature of helium plasma at high electron density $(n_e > 10^{18} cm^{-3})$ using the emissivity ratio method has been given (Griem, 2005 and Cremona, 2012). Some work has been done on homogenous plasma at low electron densities $(n_e < 10^{14} cm^{-3})$ (Rosen, 2014).

It is common practice to use the magnetic flux variable ψ as a coordinate. The parameter ψ is constant along the magnetic field lines and it can be used as a coordinate to distinguish the magnetic surfaces. $\vec{\nabla}\psi$ is a bases unit vector (in the contravariant vector representation) normal to the magnetic flux surfaces ψ. Moreover, it can be used to show the direction of the increase of the nested magnetic flux surfaces tori. The qualification of the function ψ to be a magnetic surface variable has been given and ψ is defined to be zero at the sepraratix. Also, the approximately hyperbolic nature of the magnetic field lines near the x-point of the separatrix has been proved, see Fig.1 and Fig. 3c.
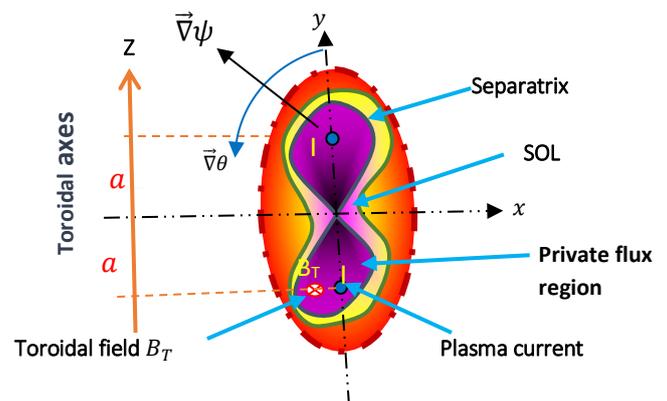

Fig. 1. Plasma cross-section with magnetic divertor configuration including Scarp Off Layer (SOL).
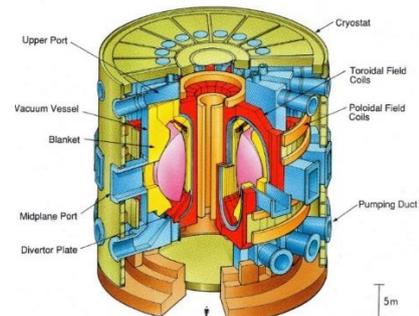

Fig. 2. International thermonuclear Experimental Reactor with Divertor Facilities, (curtesy of ITER Group).

No work that we are aware of has been published on the determination of the electron density in inhomogeneous plasmas at very low electron density ($n_e < 10^9 cm^{-3}$) such as that in tokamak divertor, see Fig. 1, and Fig. 2. The technique of measuring the electron temperature in tokamak with hyperbolic magnetic configuration (divertor) inside the Scrap off Layer (SOL) by the emissivity ratio is given (Rosen, 2014 and Alhasi, 2008), hence, the electron density can be inferred. To obtain a ratio, which is sensitive to temperature, it is necessary that the two levels are well separated in energy in their upper levels. The H_β and H_γ lines are particularly convenient for this type of plasma. Firstly, the intensity of the two lines are measured along the line of sight. Secondly, the spatial distribution of the emissivity is obtained for each particular line using the hyperbolic inversion method (Alhasi, 2007). The Abel method is applicable to plasma distributions with symmetry of a conic section, where tokamaks of circular symmetry use Backstan's method

(Backstan, 1961), and tokamaks with elliptical symmetry use Yasumoto's inversion, (Yasumoto, 1981) and tokamaks with hyperbolic magnetic lines symmetry use the so-called Alhasi technique, (Alhasi and Elliott, 1992), see Fig. 3. The result of the inversion is to yield the spectral emissivity as a function of the magnetic flux coordinate ψ from which the electron temperature can be obtained; hence we are capable of determining the electron density. The purpose of this paper is to show how the electron density is calculated. In this derivation we assume a Maxwellian distribution of electron velocities, an optically thin plasma, and an excitation distribution given by coronal type equations. The first assumption will depend on the particular plasma and should be examined in each individual case. The second and the third assumptions are easily fulfilled for the type of plasma with 2cm optical depth and electron density ($n{\sim}2.5x10^9 cm^{-3}$) respectively, (Harris, 2009; Woods, 2006).
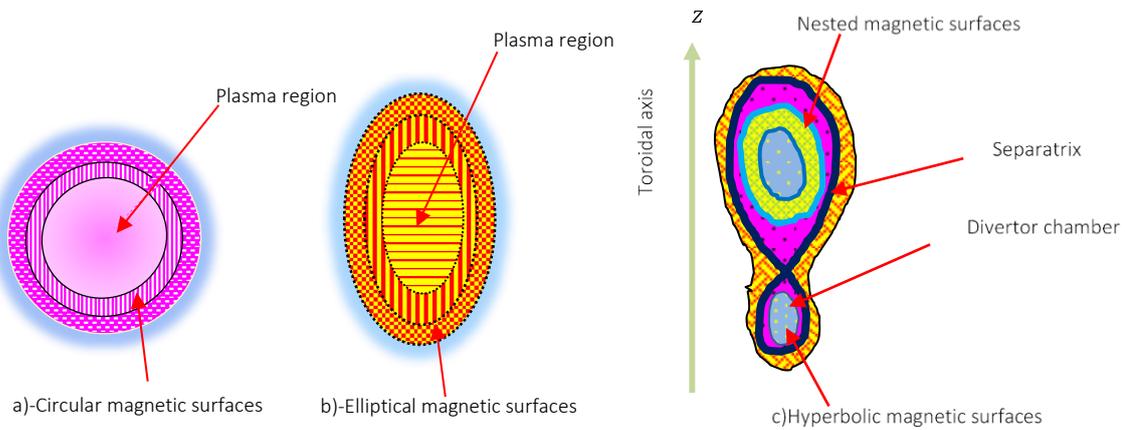

Fig. 3. Different shapes of magnetic surface configuration.

2. Flux surfaces and flux coordinates

We have to introduce that for axisymmetric equilibria, which are independent of the toroidal angle ξ, the magnetic field lines lie in nested toroidal magnetic surfaces as illustrated in Fig. 3c. The basic condition for equilibrium is that the force on the plasma is zero at all points. This requires that the magnetic force balance the force due to the plasma pressure, that is

$$\vec{j} \times \vec{B} = \vec{\nabla} p \tag{1}$$

It is clear from this equation that $\vec{B} \cdot \vec{\nabla} p = 0$. Thus, there is no pressure gradient along the magnetic field lines and the magnetic surfaces are surfaces of constant pressure. Furthermore Eq. (1) gives $\vec{j} \cdot \vec{\nabla} p = 0$, and consequently the current lines also lie in the magnetic surfaces.

It is also clear that any function $f(r)$ that satisfy the following identity $(\vec{B} \cdot \vec{\nabla}) f(r) = 0$, is constant in the magnetic surfaces and the magnetic flux surface function $\psi(r)$ is one of them, (Wesson, 1987). In the geometry of hyperbolic magnetic flux surface, the function $\psi(r)$ is related to the vector magnetic potential $\vec{A}$, which defined the shape of the magnetic field surfaces, to prove that the geometry of the field lines is depicted in Fig. 4, where ($\pm a$) are the centroids of the plasma current (I) inside the private flux chambers as illustrated in Fig. 1.

The prove is twofold, one can find the components of the magnetic field and then can drive the vector magnetic potential $\vec{A}(r)$ and the magnetic flux surface function $\psi(r)$, (Alhasi, 2018), we follow the second approach where the vector magnetic potential $\vec{A}(r)$ is obtained and then the magnetic surface function $\psi(r)$ is derived. Using the cylindrical coordinate with the toroidal ξ axis parallel to the axis $\hat{z}$ and to the plasma current (I), we can write the following vector differential equation, (Alhasi, 2018; Boozer, 2004):

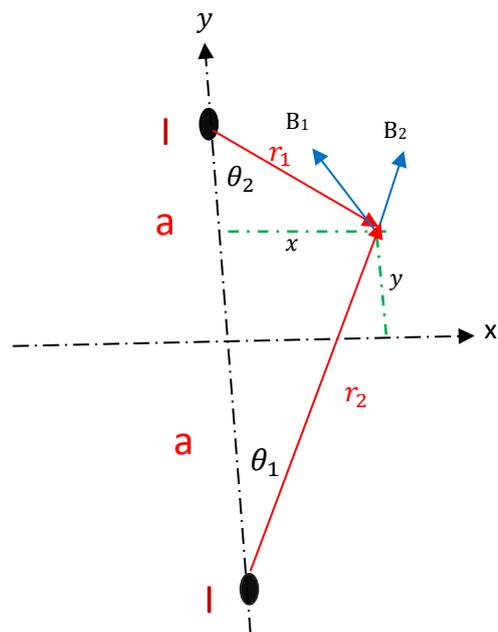$$\vec{\nabla} \times \vec{A} = \frac{\mu_0 I}{2\pi r_1} \vec{\nabla}\theta \tag{2}$$

Fig. 4. Layout geometry used to show the structure of the magnetic field components in (x, y) plane.

where r_1 is the distance from the plasma current (I), see Fig. 1 and Fig. 4. Since $\vec{B}$ possesses only θ component, only θ component of the cylindrical curl is needed.

$$\frac{\partial A_{r_1}}{\partial \xi} - \frac{\partial A_\xi}{\partial r_1} = \frac{\mu_0 I}{2\pi r_1} \tag{3}$$

It is evident that $\vec{A}$ cannot be a function of ξ, since the plasma current (I) is in the direction of ξ. Thus, the solution of the Eq. (3) is;

$$A_\xi = -\frac{\mu_0 I}{2\pi} ln r_1 + c_1 \tag{4}$$

where c_1 is a constant of integration. Since the vector magnetic potential $\vec{A}(r)$ is additive, the total contribution from both plasma region is

$$A_\xi = -\frac{\mu_0 I}{2\pi}(ln r_1 + ln r_2) + constant \tag{5}$$

Substituting for r_1 and r_2, see Fig. 4, we obtain;

$$A_\xi = \frac{\mu_0 I}{4\pi}\left(ln \frac{a^4}{(x^2 + (a-y)^2)(x^2 + (a+y)^2)}\right) \tag{6}$$

where we require the vector magnetic potential $\vec{A}(x, y)$ to vanish at the origin $(x = 0, y = 0)$ and the integration constant equal $(\frac{\mu_0 I}{2\pi} ln a^2)$. The vector magnetic potential $\vec{A}$ defined by $\vec{B} = \vec{\nabla} \times \vec{A}$ can be related to ψ. In an axisymmetric system with no variation in the toroidal direction ξ, As we have $\frac{\partial}{\partial \xi} = 0$:

$$B_x = \frac{\partial A_\xi}{\partial y} - \frac{\partial A_y}{\partial \xi} \quad and \quad B_y = \frac{\partial A_x}{\partial \xi} - \frac{\partial A_\xi}{\partial x} \tag{7}$$

which implies that

$$B_x = \frac{\partial A_\xi}{\partial y} = -\frac{\partial \psi}{\partial y} \quad and \quad B_y = -\frac{\partial A_\xi}{\partial x} = \frac{\partial \psi}{\partial x} \tag{8}$$

from which we obtain

$$\psi \equiv -A_\xi = \frac{\mu_0 I}{4\pi} ln \frac{[x^2 + (a+y)^2][x^2 + (a-y)^2]}{a^4} = \frac{\mu_0 I}{4\pi} ln\chi \tag{9}$$

ψ satisfies the identity $(\vec{B} \cdot \vec{\nabla})f(r) = 0$ as following:

$$(\boldsymbol{B} \cdot \boldsymbol{\nabla})\psi = B_x \frac{\partial \psi}{\partial x} + B_y \frac{\partial \psi}{\partial y} = B_x B_y - B_y B_x = 0 \tag{10}$$

This implies that the magnetic flux surface function ψ is constant in the magnetic surfaces and can be used as a coordinate to distinguish them.

3. Magnetic field structure of poloidal divertor

Using the expression obtained for the magnetic surfaces function $\psi(r)$, we can find the approximate form of the magnetic field topology inside the poloidal divertor. Using this definition for $\psi \equiv \frac{\mu_0 I}{4\pi} ln\chi$, we can write χ in two forms:

$$\chi \equiv \frac{[x^2+(a+y)^2][x^2+(a-y)^2]}{a^4} \quad and \quad \chi \equiv e^{\frac{4\pi\psi}{\mu_0 I}} \tag{11}$$

Since we are interested in the region inside the private flux near the x-point of the separatrix, where $y \ll a$ and the plasma current is fairly large. We can carry a series of approximations, see Fig. 1 and Fig. 4. The function $\chi(r)$ is defined as:

(a)- $\chi = 1$ implies $\psi = 0$, the separatrix.
(b)- $0 < \chi < 1$ implies $\psi < 0$, negative inside the separatrix (private flux region).
(c)- $\chi > 1$ implies $\psi > 0$, positive outside the separatrix (shared flux-region). Considering case (b) with $\chi < 1$ finding the root of x^2 from the first definition of χ in Eq. (11) and expanding using $y \ll a$ we get:

$$x^2 \cong a^2 \chi^{\frac{1}{2}}\left(1 + \frac{2y^2}{a^2\chi}\right) - (a^2 + y^2) \cong a^2\left(\chi^{\frac{1}{2}} - 1\right) + y^2 \tag{12}$$

Thus, roughly we have:

$$x^2 - y^2 \cong a^2\left(\chi^{\frac{1}{2}} - 1\right) \tag{13}$$

Using the second definition of χ in Eq. (11) and expanding the exponential under the condition $I \gg 1$, we get:

$$\chi \approx 1 + \frac{4\pi\psi}{\mu_0 I} \tag{14}$$

Taking the square roots of both sides of Eq. (14), expanding once more and substituting in the right side of Eq. (13) the magnetic surfaces near the x-point are approximately hyperbolic as:

$$x^2 - y^2 \cong \frac{2\pi a^2}{\mu_0 I}\psi \tag{15}$$

The units of ψ is (Wb/m) as deduced from Eq. (9), and the constant (a) is the centroid of the plasma column and it is related to the column shape (machine design). Most tokamaks currents range $(0.1 - 5)MA$, (Wesson, 1987). For this work, we choose $a = 0.2m$ and $I = 0.2 \times 10^6$ A, and Eq. (15) becomes:

$$x^2 - y^2 \cong \frac{2\pi a^2}{\mu_0 I}\psi = \frac{4 \times 10^{-2}}{2 \times 10^{-7} 2 \times 10^5}\psi = \psi \tag{16}$$

Therefore, in this case, we say that, the magnetic field $\vec{B}$ covers the whole surface (S) ergodically (the flux surface is densely covered by a single line); the Poincare' theorem states that" only the toroidal surface" can be covered by the nonzero vector field $\vec{B}$. Since it is a conscience of plasma equilibrium that ψ is constant on any magnetic flux surface, hence identity in Eq. (10) is applied to make ψ a magnetic surface coordinate. For those who are interested to see how the magnetic flux surface function $\psi(r) \propto r^2$ we refer them to (D'haeseleri and Hitchen, 1990).

4. Electron plasma density

To solve the Able inversion problem when the plasma is confined in tokamak with a magnetic divertor, where the magnetic field lines are now hyperbolic in shape, see Fig. 1. This requires the application of the hyperbolic inversion (Alhasi, 2007). To outline this technique, for convenience we choose the cylindrical instead of the usual toroidal coordinate for the torus cross-section. Let $\phi(y)$ denotes the relative spectral radiance of the plasma in the x direction a distance y from xz plane. A study of the relative spectral radiance from the plasma column of length $2x$ and cross-section $\Delta x \Delta z$ gives the equation, (Alhasi and Elliott 1992):

$$\phi(y)\Delta y\Delta z = \sum_{-x}^{+x} \epsilon(\psi)\Delta x\Delta y\Delta z \tag{17}$$

Viewing plasma along a single chord in x direction, normal to the direction of scan y, the plasma relative intensity $\phi(y)$ can be obtained. The function $\phi(y)$ for H_β and H_γ hydrogen lines are usually measured relative to its maximum value set by the detector system thus shows no units in its vertical axis as shown in Fig. 5.
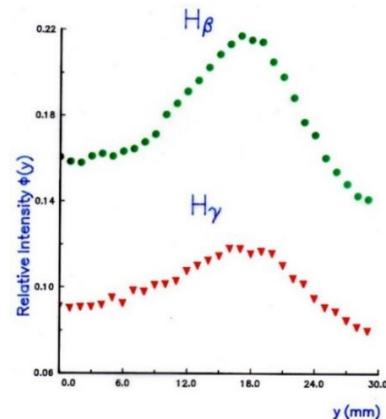

Fig.5. The relative plasma intensity $\phi(y)$ for H_β and H_γ hydrogen lines.

Starting from Eq. (17) and passing over to infinitely small volume elements and making use of symmetry about the y-axis to get:

$$\phi(y) = 2 \int_0^x \epsilon(\psi)\, dx \qquad (18)$$

Substituting the value dx resulting from Eq. (16), the following expression for the intensity is:

$$\phi(y) = \int_0^{y^2} \frac{\epsilon(\psi)dy}{\sqrt{y^2 - \psi}} \qquad (19)$$

The function $\phi(y)$ represents the integral transform of the plasma emissivity along the line of sight. The inverse transform of Eq. (19) is given (Alhasi, 2007) as:

$$\epsilon(\psi) = \frac{1}{\pi} \int_0^{\sqrt{\psi}} \frac{\left(\frac{d\phi}{dy}\right)dy}{\sqrt{\psi - y^2}} \qquad (20)$$

The integral in Eq. (20) cannot usually be performed analytically. The numerical solution of Eq. (20) is given and the α_{jk} coefficients are tabulated, (Alhasi and Elliott, 1992), the result is:

$$\epsilon_j = \frac{1}{\psi_{max}^{1/2}} \sum_{k=0}^{j-1} \alpha_{jk}\, \phi_k \qquad (21)$$

Now the plasma cross-section can be scanned to get the intensity column ϕ_k. Using the tabulated α_{jk} coefficients to obtain the emissivity column ϵ_j for each line of H_β and H_γ of Eq. (21), see Fig. 6. The transitions used are $\left(2S_{1/2} \rightarrow 4P_{3/2}\right)$, $\left(2P_{3/2} \rightarrow 4S_{1/2}, 4D_{5/2}\right)$, and $\left(2S_{1/2} \rightarrow 5P_{3/2}\right)$, $\left(2P_{3/2} \rightarrow 5S_{1/2}, 5D_{5/2}\right)$. They are the configurations for H_β and H_γ lines respectively. The emissivity ratio of these transitions is given, (Alhasi, 2007) and (Rosen, 2014) as:

$$\frac{\epsilon_\beta}{\epsilon_\gamma} = \frac{\lambda_\gamma}{\lambda_\beta} \frac{f_\beta}{f_\gamma} \left[\frac{A_\beta \sum_\gamma A_\gamma}{A_\gamma \sum_\beta A_\beta}\right] \frac{\chi_\gamma}{\chi_\beta} exp\left(-\frac{\chi_\beta - \chi_\gamma}{\kappa T_e}\right) \qquad (22)$$

The relative plasma emissivity $\epsilon(\psi)$ at the flux surfaces ψ measurements for H_β and H_γ the hydrogen line is taken relative to the maximum emissivity of the black body which is equal to one, hence no unit appears on the vertical axis, see Fig. 6.
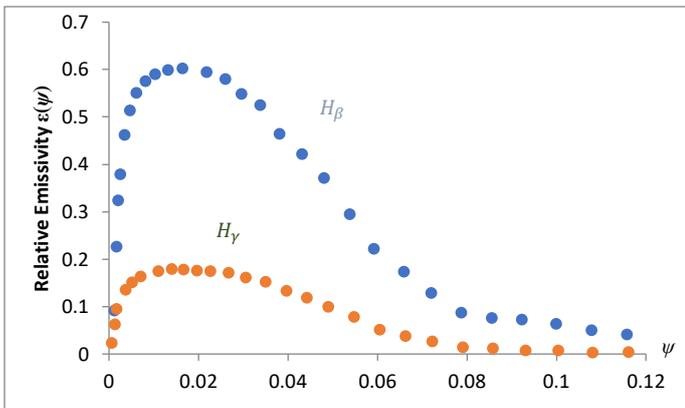

Fig. 6. The relative plasma emissivity $\epsilon(\psi)$ calculated for the H_β and H_γ hydrogen lines.

Where A_β and A_γ are the total Einstein transition probability and χ_β and χ_γ are the energy for H_β and H_γ levels in eV, and λ and f are the wavelength and frequency for each line respectively. Substituting for their tabulated values, (Wiese, 1966) and solving for T_e to have:

$$T_e = \frac{0.30}{ln\left(\frac{\epsilon_\beta}{\epsilon_\gamma}\right) - ln\left(2.7\left(\frac{A_\beta}{\sum_\beta A_\beta} \frac{\sum_\gamma A_\gamma}{A_\gamma}\right)\right)}$$

$$= \left\{\frac{0.30}{ln\left(\frac{\epsilon_\beta}{\epsilon_\gamma}\right) - ln(3.4)}\right\} \; eV \qquad (23)$$

Using this outlined technique, the temperature is measured as a function of ψ along the torus divertor, see Fig. 7. We may check the accuracy of this method by assuming that the temperature in Eq. (22) is about 10 eV. Rearranging the above expression to get the following value for the emissivity ratio:

$$ln\left\{\frac{(\epsilon_\beta/\epsilon_\gamma)}{3.4}\right\} = 0.03 \qquad (24)$$

Simplifying Eq. (24) and expanding the resulting exponential, the error in the emissivity ratio is $\Delta\left(\frac{\epsilon_\beta}{\epsilon_\gamma}\right) < 0.1\%$. Thus, to achieve a temperature measurement at the point ψ where $T_e = 10eV$, the accuracy in the emissivity ratio has to be $\leq 3\%$.
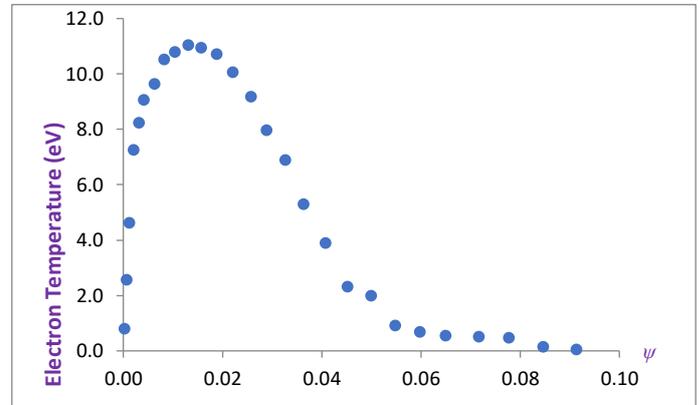

Fig. 7. The plasma electron temperature as function of the flux parameter ψ.

Now the electron temperature is secured from the emissivity ratio, Eq. (22) and if the Steady State Corona Model (SSCM) is adopted to arrive at a balance between the rate of collisional excitation from the ground level and the rate of spontaneous radiative decay (Griem, 2005), the electron density is obtained as:

$$n_e = 3.58x10^{10} T_e^{1/2} exp\left(\frac{2.324x10^3}{T_e}\right) \qquad (25)$$

For plasma with an electron temperature of about $10 \; eV$ the upper-density limit is $n_e < 1.22x10^{13} cm^{-3}$. The electron plasma density in most tokamak divertor is about $2.5x10^9 cm^{-3}$, hence the application of SSCM model is justified. Finally, to plot the electron density distribution, the values of electron temperature have to be in degree Kelvin before it is used into Eq. (24). The electron density is measured as a function of the flux parameter ψ inside the torus divertor, see Fig. 8.
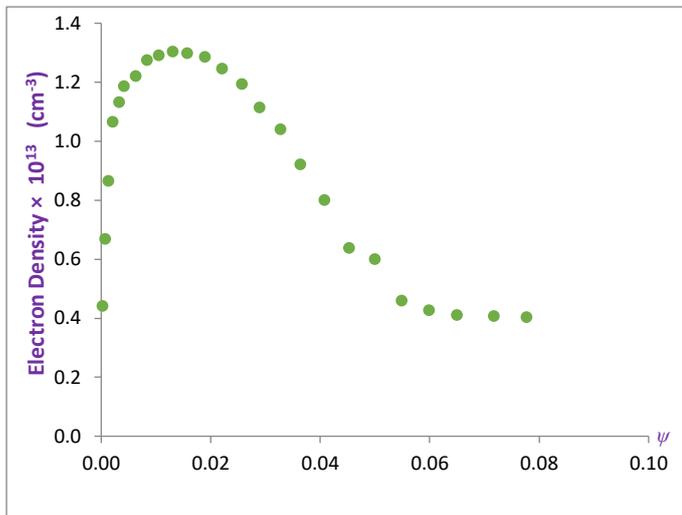
Fig. 8 The plasma electron density as a function of the flux parameter ψ.

5. Conclusion

Tokamaks use different techniques to measure the plasma density ranging from interferometry to Thomson laser scattering. One of the most powerful techniques of diagnosis is to use the scattering of electromagnetic radiation from plasma. The attractiveness of this diagnostic derives from two main features. First, it is, for all practical purposes, a non perturbing method, requiring only access of radiation to the plasma. Second, it offers the potential of determining detailed information about the distribution function of electrons' temperature and density. As it is a step of major importance, in plasma spectroscopy of cylindrically symmetric tokamaks, numerous papers have been devoted to the numerical solution of the integrodifferential Abel inversion equation, (Alhasi, 2007; Yasumoto, 1981; Bockasten, 1961). However, as pointed out in the introduction, at the present state of the art no universal method is available for every type of symmetry. Therefore, Able's inversion remains an open problem. Adopting the Steady State Corona Model (SSCM) in tokamak divertor, such as that of the International Thermonuclear Experimental Reactor (ITER). Firstly, the relative plasma intensity is measured and secondly the emissivity ratio of the H_β and H_γ lines of hydrogen plasma is calculated to obtain the electron temperature. Finally, the electron density curve is inferred by the substitution of the temperature values given by Eq. (23) into Eq. (25). The application of SSCM model is justified by the upper-density limit shown, which is above most tokamak divertor density with saving margin.

4. References

Alhasi, A.S. (2018) 'Equilibrium Studies of the Magnetic Surface function ψ of Tokamaks with Poloidal Divertor', *J. Sci.* and Technology, 5(2), pp. 16-21.

Alhasi, A. S. (2008) 'Review of Plasma Tomography on Tokamak System', *AL-NAWAH*, 9, 13, pp. 76-82.

Alhasi, A. S. (2007) 'Reconstruction of Emissivity profile by Inverting Intensity Profile in Hyperbolic Geometry Similar to ITER divertor Configuration', *J. Sci. and its App.*, 1, 2, pp. 108-116.

Alhasi, A. S. and Elliott, J. (1992) 'Plasma Diagnostics by Abel Inversion in Hyperbolic Geometry', *Plasma Phys. and Cont. Fusion*, 34, 3, pp. 367-375.

Alhasi, A. S. and Elliott J., (1992) 'Determination of Electron Temperature from the Emissivity Ratio in the UMIST Quadrupole Golux', *Plasma Phys. and Cont. Fusion*, 34, 6, pp. 947-955.

Bockasten, K., (1961) 'Transformation of observed Radiance into Radial Distribution of the emission of a Plasma', *J. of Opt. Soc. Of Am.*, 51, 9, pp. 943-953.

Boozer, A.H., (2004) 'Physics of Magnetically Confined Plasmas', *Review of Modern Phys., 76,* pp. 1071-1141.

Cremona, A., Garavaglia, S., Granucci, G., Meller, V., Minelli, D., Ricci, D., Sozzi, C., (2012) Electron temperature measurement by optical emission spectroscopy in the low-density plasma of the linear device GyM, 39th ESP Conference &16th Int. Congress on plasma physics, P4.134.

D'haeseler, W, D, W.D., Hitchen, W.N., Callen, J.D., Shohet, J.L., (1990) Flux Coordinates and Magnetic Field Structure", Spring-Verlag, London, pp. 55-93.

Griem, C. (2005) "Principles of Plasma Spectroscopy", Cambridge, pp. 258-297.

Harris, W. S., Trask, E., Roche, T., Garate, E. P., Heidbrink, W. W., McWilliams, R. (2009) 'Ion Flow Measurements and Plasma Current Analysis in the Irvine Field Reversed Configuration', *Physics of Plasma*, 16, 11, pp. 1-9 https://doi.org/10.1063/1.3265961.

Rosen, A. S., Reinke, M.L., Rice, J.E., Hubbard, A.E, and Hughes, J.W., (2014) 'Validation of x-ray line ratio for electron temperature determination in tokamak plasma', *J. of Physics B: Atomic, Molecular and Optical physics*, 47(10). DOI: 10.1088/0953-4075/47/10/105701

Yasumoto, Y. (1981) 'A New Numerical Method for Asymmetrical Abel Inversion', *IEEE Trans. Plasma Sci.* 9, 1, pp. 82-91.

Wesson. (1987), "Tokamaks"1st Ed., Clarendon press, Oxford, pp. 63-67.

Wiese, W.L., Smith M.W., Glennon B.M., (1966) "Atomic Transition probabilities, Hydrogen through Neon" NSRDS-NBS4, Vol. I

Woods, L. C. (2006) "Theory of Tokamak Transport" New Aspects for Nuclear Fusion Design, 1st ed., Wily- VCH Ver., GmbH &Co., pp. 2-4.

Woods, L. C. (1987) "Principles of Magneto plasma Dynamics", Clarendon press, Oxford, 1st ed, pp. 110-114.